Immunohistologic Assessment of Technetium-99m-MIBI Uptake in Benign and Malignant Breast Lesions

John A. Cutrone, Lisa Shane Yospur, Iraj Khalkhali, Jorge Tolmos, Alessandro Devito, Linda Diggles, Maria Perla Vargas, Paul Shitabata and Samuel French

Departments of Radiology, Pathology, and Surgery, Harbor-UCLA Medical Center, Torrance, California; Department of Pathology, National Cancer Institute, Bethesda, Maryland; and Pathology Consultants Medical Group, Torrance, California

This study was undertaken to assess the relationship between the degree of ^{99m}Tc-MIBI uptake in breast lesions and the following histologic factors: neovascularity, desmoplastic reaction, cellular proliferation and mitochondrial density. **Methods:** Forty-two patients who previously underwent MIBI breast imaging (4 false-negative, 12 false-positive, 15 true-negative, 11 true-positive) were studied. Immunohistochemical staining was performed for neovascularity (Factor VIII antigen), desmoplasia (alpha-actin antigen), mitochondrial density (mitochondrial antigen) and cellular proliferation (MIB-1 antigen). The degree of microscopic staining was correlated with region of interest measurements of MIBI uptake on scintigraphy. **Results:** There was a poor correlation between MIBI uptake and the degrees of neovascularity ($r = 0.08$, $p > 0.05$) and intracellular mitochondrial density ($r = 0.04$, $p > 0.05$) while there was a moderate correlation with cellular proliferation ($r = 0.4$, $p < 0.05$) and desmoplasia ($r = 0.55$, $p < 0.001$). **Conclusion:** The degree of MIBI uptake in breast lesions is multifactorial, but it appears to be related more to the degree of desmoplastic activity and cellular proliferation than neovascularity and mitochondrial density.

Key Words: technetium-99m-MIBI; scintimammography; angiogenesis; desmoplasia

J Nucl Med 1998; 39:449–453

Technetium-99m-MIBI, a widely used myocardial perfusion imaging agent, is frequently used for tumor imaging (*1*). At many institutions, MIBI is being investigated for its usefulness in the workup of breast lesions that are difficult to characterize mammographically (*2,3*).

MIBI localizes in the myocardium in proportion to the amount of blood flow (*4,5*). Cellular uptake in myocardial cells is related to retention of the MIBI cation by intracellular mitochondria (*6*). Mitochondrial retention of MIBI does not appear to be organ specific (*7*) and thus may account for MIBI accumulation in tumors such as breast carcinoma.

Hallmarks of breast carcinoma, like many malignancies, include increased mitotic activity of tumor cells, the development of neovascularization (angiogenesis) as a means of obtaining nutrients for growth and invasion and the development of intense fibrosis (desmoplasia). While increased mitotic activity is seen in both in situ and invasive tumors, angiogenesis and desmoplasia signal tumor invasiveness (*8,9*).

With MIBI breast scanning, as with other oncologic scintigraphic exams, the distinction between positive and negative results depends on the degree of focal radiotracer uptake in the area of suspected tumor location. Our goal in this study was to determine to what degree the MIBI uptake in various breast lesions corresponded to the traditional indicators of malignancy (angiogenesis, desmoplasia, mitotic activity) as well as the proven mechanism of MIBI uptake (mitochondrial retention).

This was performed by studying histologic specimens using immunohistochemical markers for these four processes: (1) Quantitation of angiogenesis was performed using an antibody directed against Factor VIII antigen, which is an antigen universally present within blood vessel endothelial cells. (2) For mitotic activity, an antibody to Ki-67 antigen (MIB-1 antibody) was used, which is an antigen found in cells that are actively replicating but not in those that are at rest. (3) For mitochondria, an antibody to the mitochondria itself (human mitochondrial antibody) was used. (4) For desmoplasia, an antibody to an antigen found within activated myofibroblasts (alpha actin) was chosen.

MATERIALS AND METHODS

Case Selection

Between 1992 and 1995, over 750 women at Harbor-UCLA Medical Center underwent prone MIBI scintimammography using the protocol that has previously been described (*10*). Each woman received 20 mCi (740 MBq) MIBI intravenously in the arm contralateral to the breast with the suspected abnormality identified by mammography and/or physical exam. At 5 min postinjection, planar images in the lateral projection were obtained, with the patient in the prone position, in all patients. At 60 min postinjection, lateral planar images were obtained on earlier (1993 and before) patients before this late image was dropped from our routine protocol.

Subsequent pathologic examinations in 202 patients showed 208 lesions (152 lesions by surgical excisional biopsy, 56 lesions by FNA biopsy). For the purpose of this study, the histologic slides of all 152 excisional biopsy cases were requested from the pathology archives. Cases were automatically excluded if the histologic slides could not be located or if the quantity or quality of the remaining paraffin-embedded tissue was insufficient for further study (74 cases excluded). From the sample pool of the 68 remaining cases, all 16 cases of scintigraphic misdiagnosis (12 false-positive and 4 false-negative) were selected for analysis. Of the remaining 52 cases (30 true-negative, 22 true-positive), 50% of the cases were selected randomly for further study from each group. The study was thus performed on 42 cases (4 false-negative, 12 false-positive, 15 true-negative, 11 true-positive). Correlations of the degree of MIBI uptake with histologic variables as described below were made.

Histologic Immunostaining

Histologic slides were reviewed on each of the 42 cases and the most representative section from each case was selected. Using the standard immunoperoxidase technique for the staining of formalin fixed histologic material, sections from each case were individually stained for four separate antigens: Factor VIII antigen (Polyclonal, Dako, Santa Barbara, CA) for endothelial cells of blood vessels; mitochondrial antigen (Biogenix, San Ramon, CA) for intracellular mitochondria; alpha-actin antigen (Dako, Santa Barbara, CA) for

collagen producing myofibroblasts and MIB-1 antigen (Dako, Santa Barbara, CA) for active mitoses.

For quality control, Hematoxylin and Eosin (H&E) stained slides and immunoperoxidase slides (four per case) were reviewed by one pathologist to eliminate any slides of such quality that would prevent accurate quantitations. Twenty-one of 42 slides stained for MIB-1 antigen were discarded due to poor staining and/or tissue destruction. None of the 42 slides from each of the Factor-VIII, alpha-actin and mitochondrial antigen series were discarded.

Immunostaining Interpretation

All slides were analyzed for four antigen series using the procedures described below. Two pathologists, blinded to the MIBI results, used a double-headed light microscope for simultaneous scoring of each slide. Any disagreement of a qualitative assessment was resolved by a third pathologist.

Factor VIII Antigen. Using a low microscopic magnification (25 X), the areas of the specimen exhibiting the highest degree of vascularity were identified. Using a high microscopic magnification (400 X), manual counting of brown staining of the endothelium lining blood vessels was performed. Any brown-stained endothelial cell and/or endothelial cell cluster that was clearly separate from an identified blood vessel was counted as a separate blood vessel. For each specimen, an attempt was made to count thirty 400 X microscopic fields unless 30 discrete fields could not be identified. A minimum of 15 fields were counted in each case. Results were expressed as the mean number of blood vessels per 400 X microscopic field.

MIB-1 Antigen. Using a low microscopic magnification (25 X), the areas of the specimen exhibiting the highest degree of cellularity were identified. Using a high microscopic magnification (400 X), epithelial nuclei exhibiting brown staining (i.e., actively replicating) and total nuclei were manually counted. At least 500 epithelial cells were counted in each case. Results were expressed as a percentage of total cells exhibiting positive nuclear staining.

Mitochondrial Antigen. Using a low microscopic magnification (25 X), the areas of the specimen exhibiting the highest degree of cellularity were identified. Using a high microscopic magnification (400 X), individual epithelial cells were studied. Since individual mitochondria are submicroscopic in size, a count of individual mitochondria was not possible. Intracellular brown staining aggregates of mitochondria were identifiable. A semiquantitative assessment of the percentage of epithelial cells with at least 75% of their individual intracytoplasmic volume occupied by mitochondrial staining aggregates was performed. Results were expressed accord-

TABLE 1
MIBI Uptake Spearman Rank Order Correlation

	Correlation coefficient	Number of samples (n)	p-value
Diameter of the tumor	0.23	42	>0.05
Microvessel density*	0.08	42	>0.05
Mitochondrial density†	0.04	42	>0.05
Myofibroblast density‡	0.55	42	<0.001
Proliferative index§	0.40	21	<0.05

*Microvessel density = mean number of vessels per 400× microscopic field.

†Mitochondrial density = Grade 1, < 50%; Grade 2, between 50% and 75%; Grade 3 between 75% and 99% and Grade 4 equals 100%.

‡Myofibroblast density = Grade 1, < 25% of stroma; Grade 2, between 26% and 50% of stroma and Grade 3, between 51% and 75% of stroma; Grade 4 between 76% and 100% of stroma.

§Proliferative index = % of cells in active mitosis.

TABLE 2
MIBI Uptake and Immunostaining Results in Pathology Proven Malignant Lesions

	False negatives (n = 4)	True positives (n = 11)	p-value
Diameter of the tumor	1.00 ± 0.20	3.20 ± 0.68	>0.05
MIBI	1.15 ± 0.06	2.43 ± 0.34	<0.05
Microvessel density	18.15 ± 2.14	21.94 ± 2.38	>0.05
Mitochondrial density	2.50 ± 0.50	2.73 ± 0.14	>0.05
Myofibroblast density	1.5 ± 0.50	2.36 ± 0.20	>0.05
Proliferative index	0.095 ± 0.065*	0.185 ± 0.590†	>0.05

*n = 2.
†n = 6.

ing to the following scale: Grade 1 = 1%–25% of epithelial cells; Grade 2 = 26%–50%; Grade 3 = 51%–75% and Grade 4 = 76%–100%

Alpha-Actin Antigen. Using a low microscopic magnification (25 X), the areas of the specimen exhibiting the highest degree of cellularity were identified. Using a high microscopic magnification (400 X), the percentage of stroma occupied by brown staining myofibroblasts was determined. Results were expressed according to the following scale: Grade 1 = 0%–25% of stromal area; Grade 2 = 26%–50%; Grade 3 = 51%–75% and Grade 4 = 76%–100%. It should be noted that, although alpha-actin is present not only within myofibroblasts but also within vascular pericytes, the morphologic appearance of these two cell types is sufficiently different that an accurate quantitation of myofibroblasts could be performed.

MIBI Scan Data

Region of interest (ROI) analysis was performed on each MIBI scan. Comparison of uptake in the suspected breast lesion with uptake in the corresponding region in the contralateral breast was performed and results were expressed as a tumor-to-background ratio. If no lesion could be identified visually due to apparent lack of focal uptake, the mammogram was used to determine the approximate location of the lesion to guide placement of the ROI. A target-to-nontarget ratio of < 1.4 was considered a negative result; a ratio of ≥ 1.4 was a positive result.

Statistical Analysis

All quantifiable data were analyzed using an unpaired two-tailed Student's t-test; all semiquantitative data were analyzed using the Mann-Whitney rank sum test. Spearman rank order correlation was used to determine the relationships of semiquantitative data. A statistically significant difference was considered when p values <

TABLE 3
MIBI Uptake and Immunostaining Results in Pathology Proven Benign Lesions

	False positives (n = 12)	True negatives (n = 15)	p-value
Diameter of the tumor	1.94 ± 0.29	2.32 ± 0.49	>0.05
MIBI	2.66 ± 0.32	1.07 ± 0.03	<0.01
Microvessel density	21.18 ± 1.54	19.81 ± 1.54	>0.05
Mitochondrial density	2.67 ± 0.14	2.67 ± 0.13	>0.05
Myofibroblast density	2.17 ± 0.24	1.27 ± 0.15	<0.05
Proliferative index	0.070 ± 0.023*	0.022 ± 0.01†	>0.05

*n = 7.
†n = 6.

TABLE 4				TABLE 5		

TABLE 4
MIBI Uptake and Immunostaining Results in Positives Scintimammograms

	True positives (n = 11)	False positives (n = 12)	p-value
Diameter of the tumor	3.20 ± 0.68	1.94 ± 0.29	>0.05
MIBI	2.43 ± 0.34	2.66 ± 0.32	>0.05
Microvessel density	21.94 ± 2.38	21.18 ± 1.54	>0.05
Mitochondrial density	2.73 ± 0.14	2.67 ± 0.14	>0.05
Myofibroblast density	2.36 ± 0.20	2.17 ± 0.24	>0.05
Proliferative index	0.185 ± 0.590*	0.070 ± 0.023†	>0.05

*n = 6.
†n = 7.

TABLE 5
MIBI Uptake and Immunostaining Results in Negatives Scintimammograms

	True negatives (n = 15)	False negatives (n = 4)	p-value
Diameter of the tumor	2.32 ± 0.49	1.00 ± 0.20	>0.05
MIBI	1.07 ± 0.03	1.15 ± 0.06	>0.05
Microvessel density	19.81 ± 1.54	18.15 ± 2.14	>0.05
Mitochondrial density	2.67 ± 0.13	2.50 ± 0.50	>0.05
Myofibroblast density	1.27 ± 0.15	1.5 ± 0.50	>0.05
Proliferative index	0.022 ± 0.01*	0.095 ± 0.065†	>0.05

*n = 6.
†n = 2.

0.05. Data are presented as mean ± s.e.m. All calculations were performed using SigmaStat for Windows, Version 1.0 (Jandel Corporation, San Rafael, CA).

RESULTS

Table 1 summarizes the relationship of the immunostaining results and ROI determinations in the 42 breast lesions. This shows that myofibroblast density (r = 0.55; p < 0.001) and proliferative index (r = 0.4; p < 0.05) each have a moderate and significant correlation with MIBI uptake. Microvessel density (r = 0.08, p > 0.05) and mitochondrial density (r = 0.04, p > 0.05) do not have a significant correlation with MIBI uptake. Tables 2–5 summarize the relationship of the immunostaining results and ROI determinations when each subgroup is considered individually. As seen in Table 3, a significant difference in MIBI uptake as well as myofibroblast density was seen between the false-positive and true negative groups. As seen in Table 2, a significant difference in MIBI uptake was seen between the false-negative and true-positive groups, although no differences in the histologic parameters were present. Figures 1 and 2 illustrate the significant correlation between myofibroblast density and degree of MIBI uptake.

DISCUSSION

Several centers have evaluated MIBI breast scanning for its usefulness in detecting breast carcinoma (2,3). Our group reported (11) a high sensitivity (92%) and specificity (89%) for the test. In that series of 153 pathology proven breast lesions, 11 lesions were falsely positive on MIBI scanning. That included eight lesions with various components of fibrocystic change including sclerosing adenosis and epithelial hyperplasia. The remaining three lesions were fibroadenomas. All four false-negative lesions in that series were infiltrating ductal carcinomas. The impetus for the current study is an attempt to determine whether inherent histological factors of the lesions themselves rather than technical and/or human factors could explain the cases that are misinterpreted on MIBI.

Carcinomas require angiogenesis in order to grow. Weidner et al. (12) studied angiogenesis in histologic specimens of 49 patients with invasive breast carcinoma. There was a significant difference in the number of blood vessels between the group of patients who had metastatic lesions and those who did not. Weidner et al. (12) calculated a 1.59-fold risk of metastasis for every 10 microvessels per 200 × microscopic field. In another study, Weidner et al. (13) showed that there was a significant inverse correlation between the degree of angiogenesis as measured by microvessel density and overall survival and
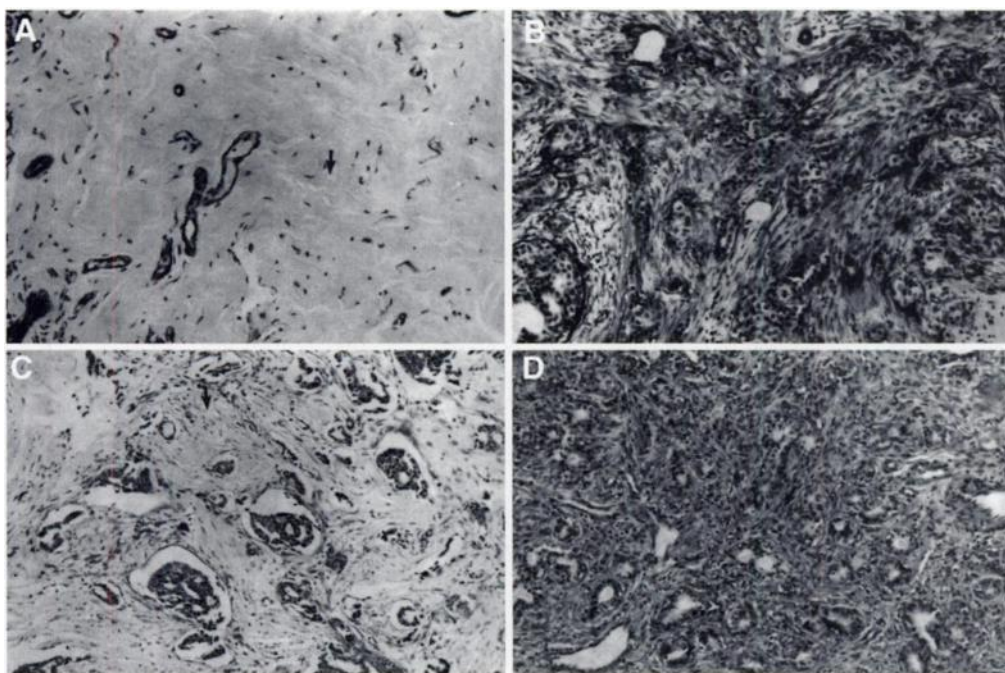
FIGURE 1. Level of active myofibroblast activity in various lesions as expressed by presence of alpha-actin antigen expression within lesion stroma in (A) true negative, (B) true positive, (C) false-negative and (D) false-positive groups. In the true negative lesion, a hyalinized fibroadenoma, note the lack of brown staining within the fibrotic stroma (arrows), which indicates the absence of active desmoplasia. Brown staining is noted only in the myofibroblasts lining blood vessel walls. The corresponding MIBI tumor-to-background ratio was 1.0. In (B), an infiltrating ductal carcinoma, there is a relatively high percentage of the stroma showing brown staining (arrows), which indicates active desmoplasia. The corresponding MIBI ratio was 2.8. In (C), an intraductal carcinoma with minimal microinvasion, there is lack of brown staining within the fibrotic stroma (arrows), which indicates the absence of active desmoplasia. The corresponding MIBI ratio was 1.0. In (D), a nonhyalinized fibroadenoma, there is abundant positive brown staining within the stroma (arrows) indicating a very high myofibroblast activity. The corresponding MIBI ratio was 4.5.
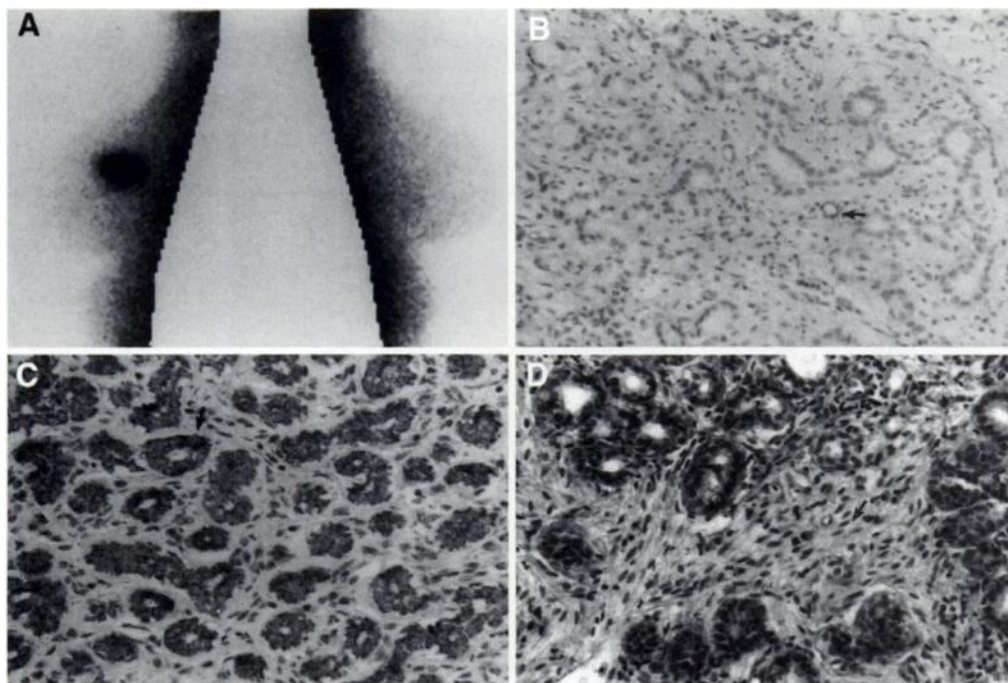
FIGURE 2. (A) False-positive scintimammogram showing marked focal MIBI uptake in a nonhyalinized fibroadenoma in the left breast. This degree of MIBI uptake was stronger than most true-positive cases. Note the lack of uptake in the normal right breast. (B) Immunohistochemical staining (200 ×) for endothelial cells and (C) mitochondria shows moderate densities, respectively. (D) Staining for activated fibroblasts showed extensive activity. By the immunoperoxidase method, the presence of focal brown staining indicates the presence of the individual antigen (arrows).

relapse free survival in breast cancer patients. Angiogenesis, however, is seen in benign as well as malignant breast lesions (*14*).

Scopinaro et al. (*15*) studied the relationship between the development of metastasis and MIBI uptake. Their data showed a significant difference in both microvessel density and MIBI uptake in patients with and without nodal metastases. They suggested a close relationship between MIBI uptake and angiogenesis. In contrast, our results show a poor overall correlation between MIBI uptake and microvascular density. While we do not dispute the significance of angiogenesis malignancy progression, our results suggest that MIBI may not be an accurate marker of this angiogenesis. The discrepancy between Scopinaro et al.'s (*15*) results and ours may be explained by the fact that they studied differences in microvessel density among a narrow group of patients with infiltrating ductal carcinoma while our study evaluated patients with a wide variety of benign and malignant lesions, all of which show some evidence of neovascularity.

Piwnica-Worms et al. (*6*) identified the mitochondria as the cellular site of MIBI retention in myocytes. Crane et al. (*7*) demonstrated that mitochondrial retention of MIBI is not organ specific. It would be expected, therefore, that lesions that are metabolically active with a high concentration of intracellular mitochondria would accumulate MIBI. In our study, we found a high concentration of mitochondria in both benign and malignant lesions and did not find a significant correlation between mitochondrial density and MIBI uptake. While we do not dispute ultrastructural studies that have placed the action site of MIBI within the mitochondria, our findings suggest that MIBI scanning is not an accurate predictor of the intracellular concentration of mitochondria. However, since our antibody stain cannot measure the physiologic changes occurring within mitochondria, it is possible that the physiologic factors that allow mitochondria to store MIBI act independently of the actual number of mitochondria within the cells.

We found a moderate correlation between the degree of cellular proliferation as demonstrated by the MIB-1 immunostaining and MIBI uptake. This is not surprising since increased mitotic activity and cellular proliferation are the hallmarks not only of invasive carcinomas but also in situ and some premalignant lesions. This may help explain why hypercellular proliferating benign lesions such as epithelial hyperplasia may produce a false-positive MIBI scan.

Hove et al. (*16*) suggested that the reactive neoplastic stroma, rather than the carcinoma itself, may be the reason MIBI accumulates in breast malignancies. Our data lend support to their claim. We found a moderate correlation between the level of myofibroblast activity and the level of MIBI uptake. Three of 4 false-negative lesions and 12 of 15 true-negative lesions showed very low (Grade 1) myofibroblast activity while only 3 of 12 false-positive and 1 of 11 true-positive lesions showed Grade 1 myofibroblast activity. Included in the group of true-positive lesions that showed very active (Grade 3) myofibroblasts were two patients with ductal carcinoma in situ (DCIS) in whom direct invasion of the tumor cells could not be detected even in retrospect. Thus, MIBI uptake may be an early indicator of the desmoplastic response. Whether this desmoplasia in DCIS is indicative of the early breakdown of the basement membrane (i.e., early invasion) is unknown. The relationship between MIBI accumulation and desmoplastic activity is promising and should be further explored.

CONCLUSION

None of the four factors studied in this article has a strong correlation with the degree of MIBI uptake. It is probable that the degree of uptake is multifactorial, with tumor replication and desmoplastic activity being more important than angiogenesis and intracellular mitochondrial density. While our study does not help explain false-negative MIBI results, in part due to the small number of available cases, it offers insight into the false-positive scans.

ACKNOWLEDGMENTS

REFERENCES

1. Abdel-Dayem HM, Scott AM, Macapinlac HA, El-Gazzar AH, Larson SM. In: Freeman LM, ed. *Annual Nuclear Medicine 1994*. New York: Raven Press, 1994: 181–234.

2. Taillefer R, Robiduox A, Lambert R, Turpin S, LaPerriere J. Technetium-99m-sestamibi prone scintimammography to detect primary breast cancer and axillary lymph node involvement. *J Nucl Med* 1995;36:1758–1765.

3. Kao CH, Wang SJ, Liu TJ. The use of technetium-99m methoxyisobutylisonitrile breast scintigraphy to evaluate palpable breast masses. *Eur J Nucl Med* 1994;21:432–435.

4. Okada RD, Glover D, Gaffney T, Williams SJ. Myocardial kinetics of technetium-99m-hexakis-2-methoxy-2-methylpropsyl-isonitrile. *Circulation* 1988;77:491–498.

5. Mousa S, Cooney J, Williams SJ. Relationship between regional myocardial blood flow and the distribution of ^{99m}Tc-sestamibi in the presence of total coronary artery occlusion. *Am Heart J* 1990;119:842–847.

6. Piwnica-Worms D, Kronauge JF, Chiu ML. Uptake and retention of hexakis(2-methoxyisobutylisonitrile) technetium (I) in cultured chick myocardial cells: mitochondrial and plasma membrane potential dependence. *Circulation* 1990;82:1826–1838.

7. Crane P, Laliberti R, Heminway S, Thoalen M, Orlandi C. Effect of mitochondrial viability and metabolism on Tc-99m sestamibi myocardial retention. *Eur J Nucl Med* 1993;20:20–25.

8. Horaker, Russel L, Klenk N. Angiogenesis, assessed by platelet/endothelial cell adhesion molecule antibodies, an indicator of node metastases and survival in breast cancer. *Lancet* 1992;340:1120–1124.

9. Visscher DW, DeMattia F, Ottosen S, Sarkar FH, Crissman JD. Biologic and clinical significance of basic fibroblast growth factor immunostaining in breast carcinoma. *Modern Pathol* 1995;8:665–670.

10. Diggles L, Mena I, Khalkhali IJ. Technical aspects of prone dependant breast scintimammography. *J Nucl Med Technol* 1994;22:165–170.

11. Khalkhali I, Cutrone JA, Mena IG, et al. Scintimammography. The complementary role of Tc-99m sestamibi prone breast imaging for the diagnosis of breast carcinoma. *Radiology* 1995;196:421–426.

12. Weidner N, Semple JP, Welch WR, Folkman J. Tumor Angiogenesis and metastasis-correlation in invasive breast carcinoma. *NEJM* 1991;324:1–8.

13. Weidner N, Folkman J, Pozza F, et al. Tumor angiogenesis: a new, significant, and independent prognostic indicator in early-stage breast carcinoma. *J Natl Cancer Inst* 1992;340:1875–1887.

14. Obrenovitch A, Monsigny M. Angiogenese tumorale. *Pathol Biol* 1986;34:189–201.

15. Scopinaro F, Schillaci O, Scarpini M, et al. Technetium-99m-sestamibi: an indicator of breast cancer invasiveness. *Eur J Nucl Med* 1994;21:984–987.

16. Hove M, Leonard MH, Villanueva-Mayer J, Cowan DF. Histopathologic correlates of ^{99m}Tc-sestamibi scanning in the breast [Abstract]. *Modern Pathol* 1995;19A.

Fluorine-18-Fluorodeoxyglucose PET Versus Thallium-201 Scintigraphy Evaluation of Thyroid Tumors

Hidemasa Uematsu, Norihiro Sadato, Toshio Ohtsubo, Tatsuro Tsuchida, Satoshi Nakamura, Katsuya Sugimoto, Atsuo Waki, Norio Takahashi, Yoshiharu Yonekura, Gota Tsuda, Hitoshi Saito, Nobushige Hayashi, Kazutaka Yamamoto and Yasushi Ishii

Department of Radiology, Biomedical Imaging Research Center, and Department of Otolaryngology, Fukui Medical School, Fukui, Japan

To determine whether PET could help differentiate malignant from benign thyroid tumors, ^{18}F-fluorodeoxyglucose (FDG) accumulation and ^{201}Tl scintigraphy were examined relative to histological diagnosis. **Methods:** Nodular thyroid lesions in 11 patients were evaluated before surgical resection. Static PET scanning with 370 MBq FDG was done for 20 min (from 40 to 60 min postinjection) in all patients, and standardized uptake values (SUVs) in these lesions were calculated. In addition, eight patients were evaluated with dynamic PET scan up to 60 min postinjection, and the lesions were further evaluated using graphical analysis. Thallium-201 delayed images were visually evaluated in 10 patients. **Results:** Four of 11 nodules were well-differentiated papillary carcinoma, another five were benign follicular adenomas, one was a multinodular goiter and another a case of chronic thyroiditis that was proved not to contain a nodule. Time-activity curves of FDG uptake showed different patterns in malignant and benign tumors. In the malignant tumors, FDG uptake increased with time after the tracer injection. By contrast, FDG uptake in benign tumors gradually decreased. With use of a cutoff value of 5.0 mg/ml for SUV and 10 μl · min^{-1} · ml^{-1} for Kc (K complex value determined using the linear fitting of the time-activity curve of FDG accumulation), all of the four malignant nodules and the six benign nodules were separated correctly. Chronic thyroiditis had high SUV in the malignant range. Of the four patients with thyroid carcinoma, the delayed ^{201}Tl images revealed a slightly higher or equal uptake to background activity. In a patient with chronic thyroiditis, the delayed ^{201}Tl images revealed diffuse accumulation higher than background activity. **Conclusion:** FDG-PET is superior to ^{201}Tl in differentiating malignant from benign tumors. Both SUVs and Kc values were useful indexes for this discrimination. Although careful evaluation is needed for chronic inflammatory lesions, this technique appears to be useful in evaluating thyroid nodules.

Key Words: thyroid tumors; PET; thallium-201 scintigraphy; fluorine-18-fluorodeoxyglucose

J Nucl Med 1998; 39:453–459

Because surgical resection is the effective treatment for thyroid tumors, preoperative differentiation between malignant and benign nodules is essential. Thyroid tumors are usually evaluated before surgery by means of clinical examination, sonography, computed tomography (CT) and fine-needle aspiration biopsy (1).

Sonography is generally the first choice for the evaluation of thyroid morphology because of its sensitivity for small nodule detection (1). The combination of sonography and fine-needle aspiration biopsy is routine in many centers. The sensitivity and specificity of scintigraphy with solitary thyroid nodules were 100% and 5.5%, respectively, whereas those of fine-needle aspiration biopsy were 100% and 91.2%, respectively (2).

In spite of these attributes, fine-needle aspiration biopsy has limitations. Accuracy depends on the skill and experience of the operator and the cytopathologist. Some benign adenomas are difficult to distinguish from malignancies (3). Follicular adenomas are particularly difficult to distinguish from well-differentiated follicular cancer. This distinction is made on the basis of whether there is capsular invasion and is difficult even on permanent histopathological sections. To improve diagnostic accuracy further, additional methods of evaluation are needed.

Although conventional radiography such as CT scanning and magnetic resonance imaging (MRI) can sometimes be used effectively, it often cannot accomplish clear, quick determina-